Simple Fabrication of Paper-like Graphene Oxide for use as Saturable Absorber in Q-switching of Fiber Laser

Simple Fabrication of Paper-like Graphene Oxide for use as Saturable Absorber in Q-switching of Fiber Laser

Yuen-Kiat Yap[1,2*], Fauzan Ahmad[3], Wu-Yi Chong[1], and Harith Ahmad[1,4]

[1] *Photonics Research Centre, University of Malaya, 50603 Kuala Lumpur, Malaysia*
[2] *Heriot-Watt University Malaysia, Precinct 5, 62200 Putrajaya, Malaysia*
[3] *Department of Electronic System Engineering, Faculty of Engineering, University of Technology Malaysia, 54100 Kuala Lumpur, Malaysia*
[4] *Physics Department, Faculty of Science, University of Malaya, 50603 Kuala Lumpur, Malaysia*
[*] *Corresponding author. E-mail: yapyuenkiat@yahoo.com*

Received: Oct. 28, 2020; Accepted: Jan. 22, 2021

The rise of graphene has made its derivatives a much sought-after research in nano-material science. One of which that has attracted substantial interest is graphene oxide. Due to its simple top-down synthesis and bandgap tunability, graphene oxide is suited in optoelectronics and photonics applications. Foil or paper-like graphene oxide possesses excellent mechanical strength especially. In this work, we demonstrated a home-made, paper-like graphene oxide for Q-switching operation in a ring erbium-doped fiber laser. The raw material was synthesized using simplified Hummers' method, and subsequently by simple filtration. The free-standing, orderly stacked material is about 6.5 nm thick, corresponding to about 6−7 layers of uniform sheets. The paper-like material was then transferred directly to a fiber ferrule and sandwiched between two connectors via a fiber adapter. Q-switched pulses were observed when the pump power of the ring laser was increased to about 68 mW. The Q-switched fiber laser has maximum repetition rate, pulse energy, pulse width and average power of 21.5 kHz, 52 nJ, 3.8 μs and 1.1 mW respectively.

Keywords: Grapheme oxide, Nano-material, Pulsed fiber laser, Q-switched, Repetition rate, Pulse width

http://dx.doi.org/10.6180/jase.202108_24(4).0007

1. Introduction

Graphene oxide (GO) is a two-dimensional nano-material derived from graphene. It is covalently decorated with oxygen containing functional groups with a mixture of chemically tunable sp^2 and sp^3 hybridized carbon atoms, making it to have flexible bandgaps, acting like a semi-metal [1]. GO started to attract much attention ever since the up-swing of graphene-related research more than a decade ago. Due to its bandgap tunability, manipulation of the relative fraction of the sp^2-hybridized domains is possible, enabling customization of its optical properties for photonics and optoelectronics applications [2]. Typically for ultrafast lasers applications, graphene has appeared to be a exemplary saturable absorber (SA) for pulsing laser, owing to its many advantages such as wideband and tunable operation, ultrafast recovery time, large absorption of incident light per layer and cost effective [3]. Traditionally, GO serves as a precursor for graphene. When compared to graphene, it is more straight forward to synthesize, process and integrate into devices at ease with readily available thin-film electronic techniques [4]. Besides, GO has better water-solubility while preserving its unique non-linear optical characteristics. It has been shown that GO possesses fast energy relaxation of hot carriers and strong saturable absorption too, which is comparable with that of graphene's [5]. In fact, there are many works done on using GO or GO related materials as SA for pulsing lasers, and the results are commendable [6–9].

On the other hand, the discovery of carbon nanotubes brought about bucky paper [10] which possesses good mechanical strength [11–14]. Liu et al. demonstrated that, through proper filtering, SWCNT suspension can form a

free-standing foil-like material [10]. Dikin et al. successfully produced paper-like GO by vacuum filtration of colloidal GO sheets through a membrane filter [15]. All these enhanced carbon-related materials are suited for many applications such as protective shield, structural composite, resistive membranes and water-proofing coating [15]. The unique properties also correspond to the requirement of SA – the material must be robust to withstand high intensity and have optimum interaction with light. It should also remain sturdy for a prolonged period on its substrate.

Most works that use GO sheets or flakes to fabricate a passive SA device is usually accompanied by a host material, such as polymer composite and quartz [16, 17]. While this makes the material mechanically strong; the preparation process is complex and tedious, with the necessity of precise control of certain synthesis parameters, such as solution's concentration, mixing ratio and exfoliation time. Besides, the incorporation of host materials could bring about substantial power loss to the device. Exploiting the strength and stability of paper-like carbon materials as reported in refs [11–15], in this work, we attempt to produce a paper-like GO material by simple filtration method. Subsequently, the as-prepared GO paper was assembled into a all-fiber format passive SA device by directly transferring it onto a fiber ferrule end face. Its viability in pulsing laser was investigated using a ring erbium-doped fiber laser (EDFL) setup. We successfully achieved pulsing in the Q-switched regime − with maximum repetition rate and pulse energy of ∼22 kHz and ∼52 nJ respectively. To the best of our knowledge, this is the first fully home-made paper-like graphene related material based Q-switched fiber laser ever demonstrated.

2. Material Preparation and Characterization

GO was synthesized using a simplified Hummer's method, summarized in Fig. 1a. Oxidation of graphite was carried out by mixing H_2SO_4:H_3PO_4 (320:80 mL), graphite flakes, and $KMnO_4$ (18 g) using a magnetic stirrer. After mixing all the materials slowly, the mixture was stirred for 3 days to allow the oxidation of graphite. Later, H_2O_2 solution was added to stop the oxidation process. The graphite oxide formed was washed three times with 1M of HCl aqueous solution followed by repetitive washing with deionized water until a pH of 4˜5 was achieved. The washing process was carried out using simple decantation of supernatant via a centrifugation technique with a centrifugation force of 10,000 g. During the washing process with deionized water, the graphite oxide experienced exfoliation, which resulted in the thickening of the solution, forming a GO gel. The whole process was carried out without any temperature control, neither increasing nor decreasing the temperature. Foil-like GO is fabricated by filtration of the GO gel using a filter paper. The purpose of the filter paper is to ensure a directional steady flow of the solution where the GO sheets can be assembled into a well-ordered structured. 10 ml of the solution was filtered, after which it was left to dry at room temperature for a day, forming a thick GO sheet (Fig. 1b) The as-synthesized GO was characterized using a UV-visible-infrared spectrophotometer (*Perkin − Elmer*1050) and Raman spectrometer (*Renishaw inVia Raman Microscope*). To confirm the formation of paper-like material, the GO was examined carefully using a field emission scanning electron microscope (*FESEM – JSM 7600 F*) and X-ray diffractometer (XRD - *BTX Benchtop X-ray Diffraction/X-ray Fluorescence*, Cu target with Kα radiation, X-ray wavelength $\approx$ 1.572 Å, operating at a tube voltage of 40 kV).

3. Experimental setup of a ring erbium-doped fiber laser

For pulsed laser study, a ring EDFL was set up as shown in Fig. 2. The SA device was fabricated by cutting a small part of the GO paper (2 × 2 mm^2) and sandwiching it in between two FC/PC fiber adapters and inserted into the ring laser resonator. The insertion loss of the SA was measured to be around 3.5 dB at 1550 nm. The polarization controller (PC) is to maintain the polarization state of the light, thus improving output pulse stability. The resonator's length is ∼12.7 m.

4. Results

4.1. Characterization results

Fig. 3 shows the UV-Visible-NIR absorption spectrum of GO. An absorption band was observed at 228 nm of excitation, with absorbance intensity of briefly 2.29. This result is in close proximity to that of graphite oxide as reported in [18]. The strong absorption band is due to the $\pi \rightarrow \pi^*$ transitions of aromatic $C = C$ bonds. The plot below 200 nm can be ignored, due to fluctuations in baseline measurement. A small 'shoulder' is observed at ∼300 nm. We attribute this to the $n \rightarrow \pi^*$ transitions of $C = O$ bonds.

Fig. 4 shows the Raman spectrum of the GO. The *D* peak (∼1353 cm^{-1}) arises from the doubly resonant disorder-induced mode due to the stretching of $C - C$ bond; the *G* peak (∼1605 cm^{-1}), a doubly degenerate phonon mode due to the first order scattering of the E_{2g} phonon of sp^2 *C* atoms [19] at the Brillouin zone center, and the 2*D* overtone peak (∼2715 cm^{-1}) [19–22]. The *D* peak is indicative of significant structural disorder due to the *O*-incorporation.

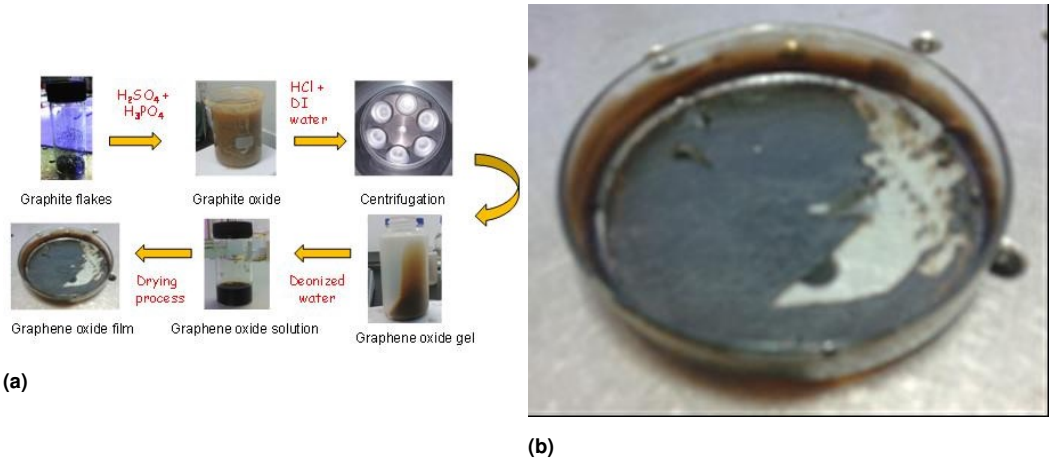

Fig. 1. (a): Simplified Hummers' method of GO synthesis and (b) GO paper formed after filtration.

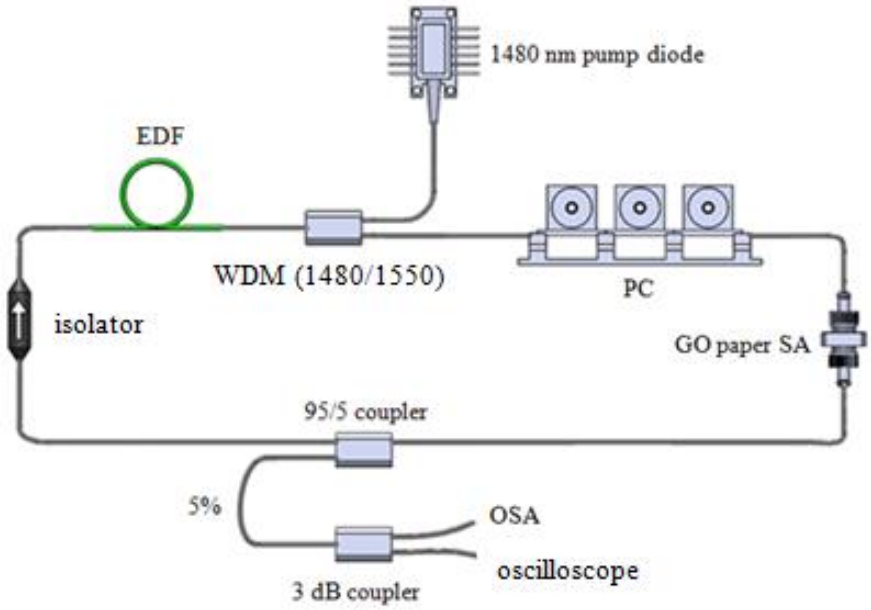

Fig. 2. A ring EDFL configuration. WDM: wavelength division multiplexer, OSA (optical spectrum analyzer).

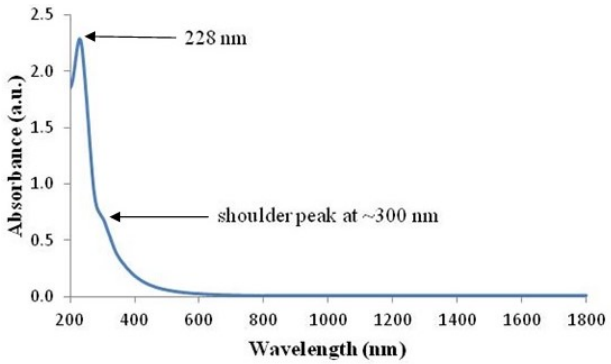

Fig. 3. UV-Vis-NIR absorption spectrum of the GO.

It is related to the size of the in-plane sp^2 domains [5].The increase of the D peak intensity indicates forming more sp^2 domains. The relative intensity ratio of both peaks (I_D/I_G) is a measure of disorder degree and is inversely proportional to the average size of the sp^2 clusters [5, 23]. Our results show a value of 0.88 for I_D/I_G, similar to that of [24]. The 2D band that originates from a two phonon double resonance Raman process is indicative of crystalline graphitic materials.

Fig. 5a shows a close-up examination of the GO using FESEM. After filtration, it shows an orderly layered GO sheets, verifying the formation of GO paper [15].

Fig. 5b shows the XRD results of the GO paper. The highest peak (8.9°) in the spectrum of a typical GO paper

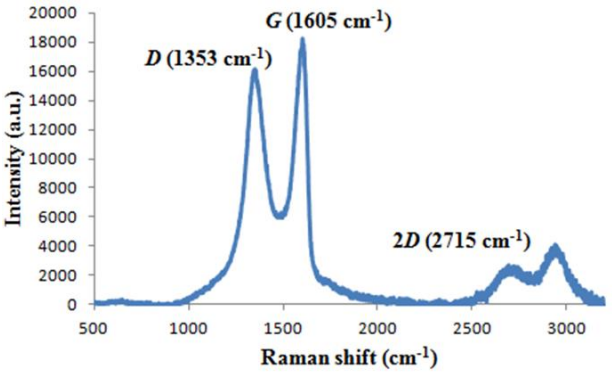

Fig. 4. Raman spectrum of the GO

corresponds to a layer to layer of distance (d-spacing) of about 1 nm, using Bragg's Law of XRD, indicating the presence of a large number of water molecules intercalated in the GO sheets, as reported by [25] and [26]. The measured distance could be attributed to an approximately one molecule thick layer of water that is presumably hydrogen-bonded between the GO sheets. Since GO itself is an allotrope of carbon whose structure is one-atom-thick planar sheets of sp^2-bonded carbon atoms, which has nano-scale dimensions, the measured dimension of the orderly stacked GO sheets that assemble a paper material can be calculated using Debye-Sherrer equation, given by

$$\tau = \frac{K\lambda}{\beta cos\theta}$$

where τ is the average size of the crystalline domains, is the shape factor, λ is the X-ray's wavelength, β is the line broadening at full wave half maximum intensity of the X-ray diffraction peak (in radian) and θ is the Bragg's angle. Assuming a crystallite structure of graphite and taking K to be 0.94, the mean dimension of the GO paper was found to be about $\sim$6.9 nm, which corresponds to about 6$-$7 stacked GO sheets.

4.2. Q-switched fiber laser performance

When the pump power of the ring laser was increased to $\sim$68 mW, Q-switched pulses were observed. The optical spectrum of the Q-switched pulses generated is shown in Fig. 6. It can be seen that there are two distinct peaks present - 1562.7 nm and 1563.1 nm, possibly due to inhomogeneous broadening of the EDF used $-$ a measure of the various sites in which an ensemble of erbium ions can be located. This means the laser-active erbium ions in the EDF used are at different lattice locations, causing the ions to interact with different wavelengths components.

Fig. 7 shows the evolution of the optical spectrum when the pump power was increased from $\sim$100 mW to $\sim$150 mW. It is obvious that the spectrum broadens as the pump power increases. The multi-peak structure superposed on the broadened Q-switched spectrum indicates the generation of several longitudinal modes in the resonator, believed to be caused by the resonator's birefringence [27]. This is expected of a Q-switched laser pulse due to modulation of the Q factor. Also, there are non-linear losses in the SA used, as GO has parametric non-linearities in the third order. This causes gain saturation, leading to optical spectrum broadening.

To further confirm the Q-switching operation, the pump power of was varied from 68 mW to the maximum available power, which is 150 mW for this setup. The time period (i.e repetition rate) scales linearly with the pump power, as shown in Fig. 8a. This is a typical characteristic of Q-switched lasers $-$ the repetition rate depends on pump power [28]. As pulse generation depends on modulation of the SA, when higher pump power is available, more gain is provided to saturate the SA. The repetition rate varies from 15.6 kHz to 21.5 kHz, giving a linear relationship with a gradient of about 0.1 kHz/mW. The average output power also increases in a similar manner from 0.2 mW to 1.1 mW, averaged at 0.01 kHz/mW for a pump power range of 68 mW to 150 mW. We believe the repetition rate and the average power can increase further; in our case, it's only limited by the available pump power. Fig. 8b shows the pulse train as measured by oscilloscope at maximum available pump power of 150 mW.

The pulse width and pulse energy as a function of pump power are shown in Fig. 9a. The pulse width decreases with increased pump power in the stable Q-switched operation regime. In details, the pulse width seemed to decrease rapidly as the pump power was increased, dropping from a maximum value of 21.3 μs to approximately 12.1 μs. This gives an initial change averaged at about -1.0 μs/mW. Subsequent increase in the pump power ($\sim$82 mW onward), on the other hand, does not lead to such a drastic drop in the pulse width, with the narrowest pulse width obtained being 3.8 s at maximum pump power of 150 mW $-$ averaged at about -0.1 μs/mW or $\sim$10% of the initial gradient for this range. We attribute this to the saturation of the upper energy level of the erbium ions at higher pump power. At lower pump power, the saturation level is relatively low. Increasing the pump power provides more photons to drench the ions. High gain is initiated in a relatively shorter time, accelerating the bleaching of the SA. Also, the laser resonator is not optimized, so chromatic dispersion could possibly bring about substantial pulse broadening. Moreover, at higher pump powers, the non-linear losses of the SA would be more significant, which could make the

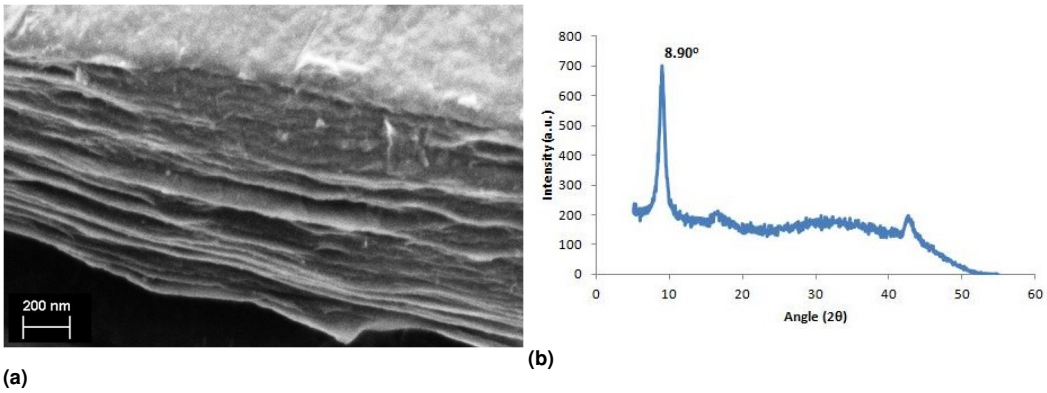

Fig. 5. (a) FESEM image and (b) XRD spectrum of the GO.

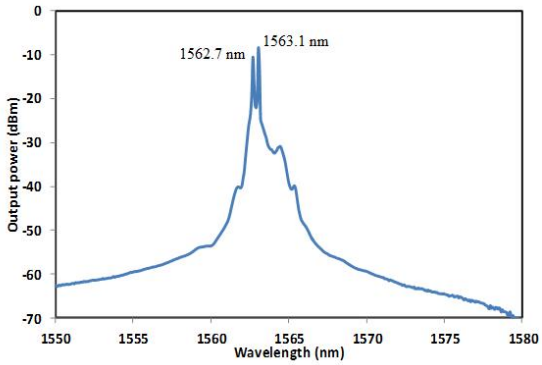

Fig. 6. Optical spectrum of the Q-switched EDFL.

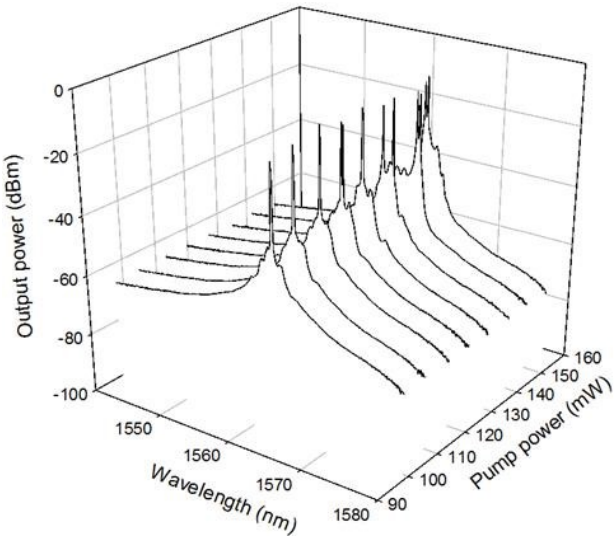

Fig. 7. Evolution of the OSA for pump power of ∼98 mW to ∼150 mW.

pulses even more sensitive to chromatic dispersion.

As for energy per pulse, seen from Fig. 9a as well, it increases monotonically from ∼15 nJ (pump power of 68 mW), to ∼52 nJ (pump power of 150 mW). Generally, shorter pulses and higher pulse energy can be achieved by having a shorter laser resonator, high-gain fiber, cladding-pump fiber and optimizing the coupling ratio [29]. Fig. 9b shows the single pulse envelope obtained at a pump power level of 150 mW, measured at full-width half-maximum (FWHM).

It is commonly known that exposure of GO to light will lead to increase in temperature and bring about reduction of GO to reduced graphene oxide, as reported by many authors of different research groups [30–33]. However the Q-switching performance of the current setup is stable throughout the entire range of parameters being tested. Guo et al. has reported on reduction of GO by continuous wave (CW) infrared (IR) light, which is the closest to the light occurring in this work [34]. The group proposed a mechanism for reduction of GO by photo-thermal effect. Significant temperature increase was observed in a ∼1 μm thick GO film when it was exposed to CW IR light. In this work, the GO paper SA used is less than 10 nm in thickness and the duty cycle of the pulsed laser is less than 10%. Therefore, we believe absorption of light by the GO paper SA is not significant to induce substantial temperature rise necessary for photo-thermal reduction of GO.

Table 1 shows the summary of some other works that are closely related to ours. Refs [35] and [36] used commercially available GO and provided only micrograph of the GO placed directly onto a fiber ferrule end face. The deposition method was assisted by index matching gel, which possibly reduces insertion or return loss, leading to lower Q-switched threshold. The laser configuration in these works is also different from that of ours (for e.g ref [35] included a short length of photonic crystal fiber to generate a dual-wavelength laser), so it is currently impossible to objectively evaluate the performance. It is worth noting that our proposed Q-switched laser's performance

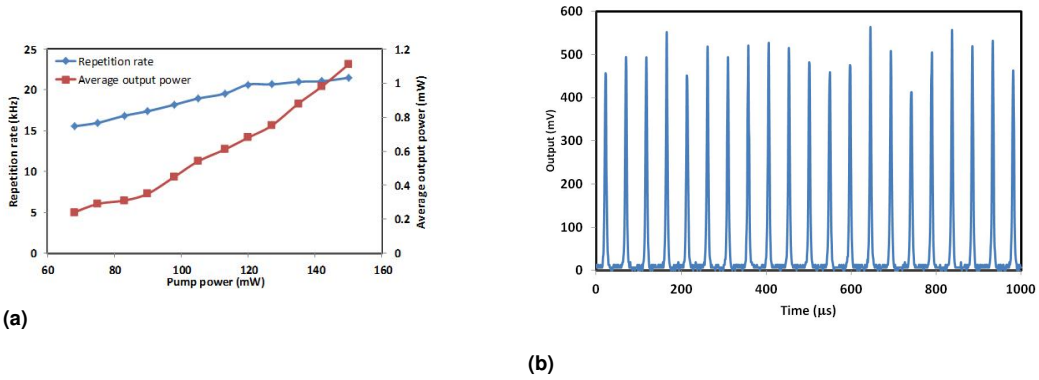

Fig. 8. (a) Repetition rate and average power of the Q-switched laser as a function of pump power and (b) oscilloscope trace of the output pulse at 150 mW of pump power.

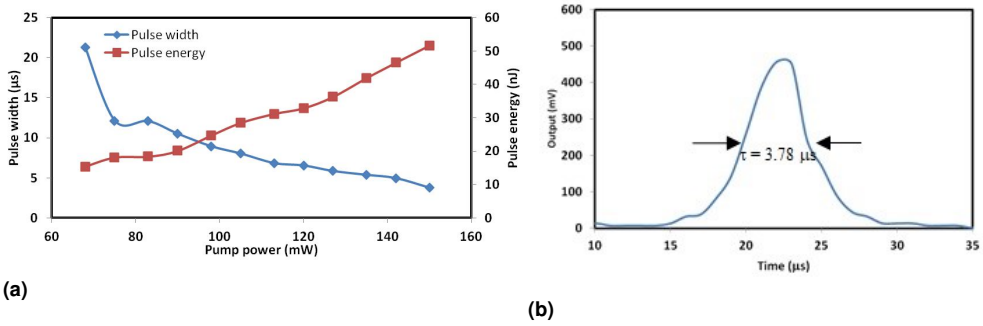

Fig. 9. (a) Pulse energy and pulse width as a function of pump power and (b) single pulse trace measured at full-width half-maximum (FWHM) at maximum pump power of 150 mW.

Table 1. Summary of GO paper based Q-switched fiber lasers.

Material preparation	Q-switched threshold	Maximum average power	Maximum pulse energy	Maximum repetition rate	Narrowest pulse width	Ref.
Commercial	∼53 mW	∼0.1 mW	∼2.6 nJ	∼31 kHz	∼7.0 μs	[35]
Commercial	∼66 mW	∼0.5 mW	∼17 nJ	∼31.5 kHz	∼14.0 μs	[36]
SHM-SFFP*	68 mW	1.1 mW	52 nJ	21.5 kHz	3.8 μs	Our work

*SHM-SFFP – Simplified Hummers' method followed by simple filtration using filter paper.

outshines the laser's performance in these two references in terms of average power, pulse energy and pulse width. We attribute this to the relatively higher saturation intensity of the GO paper SA used in our work as evidenced by the higher threshold pump power required to achieve Q-switching. With higher saturation intensity, higher gain is required to quench the upper energy level of the SA. This increases the population inversion, and brings about higher energy extraction to generate pulses with higher energy. Also, higher population inversion initiates fast energy extraction at higher intensity once Q-switching occurs, facilitating shorter pulse width. Comparatively, though these are achieved at the expense of the pump power; it indicates the potential of up-scaling, especially the pulse energy and average power, where giant pulses are desirable in specific applications such as dermatology, ophthalmology and metrology [37–39]. In our case, however, it should be noted that the potential of up-scaling may be limited by the susceptibility of the GO paper SA to photo-thermal reduction at higher laser power levels, which may cause instability

to the output pulse or quench the Q-switching operation.

5. Conclusion

We have fabricated a paper-like GO material using simple filtration. The formation of GO paper is confirmed by FE-SEM and XRD characterization results. The GO paper is transferred directly onto a fiber ferrule end face to assemble a simple passive SA device. The device has a insertion loss of 3.5 dB. When it is inserted into a ring EDFL, Q-switched pulses were observed at a diode pump power of 68 mW. The repetition rate, average output power and pulse energy scales linearly with the pump power, with a maximum of 21.5 kHz, 1.1 mW and 52 nJ achieved respectively. The pulse width decreases with increasing pump power, down to a minimum of 3.8 μs achieved in this work. We believe shorter pulse width and higher pulse energy could be enabled by using high gain or cladding-pump fiber, optimizing the laser resonator design and coupling ratio. On-going work will include improving the thermal threshold of the GO paper, layer/thickness control and understanding the interplay between different laser parameters.

6. Acknowledgement

This work is supported by the Ministry of Education of Malaysia under the Fundamental Research Grant Scheme (FRGS/1/2018/STG02/HWUM/02/2).

References

[1] Ji Won Suk, Richard D. Piner, Jinho An, and Rodney S. Ruoff. Mechanical properties of monolayer graphene oxide. *ACS Nano*, 4(11):6557–6564, nov 2010.

[2] Ayrat M. Dimiev and James M. Tour. Mechanism of graphene oxide formation. *ACS Nano*, 8(3):3060–3068, mar 2014.

[3] Zhipei Sun, Tawfique Hasan, Felice Torrisi, Daniel Popa, Giulia Privitera, Fengqiu Wang, Francesco Bonaccorso, Denis M. Basko, and Andrea C. Ferrari. Graphene mode-locked ultrafast laser. In *ACS Nano*, volume 4, pages 803–810, feb 2010.

[4] Goki Eda and Manish Chhowalla. Chemically derived graphene oxide: Towards large-area thin-film electronics and optoelectronics, jun 2010.

[5] Xin Zhao, Zhi Bo Liu, Wei Bo Yan, Yingpeng Wu, Xiao Liang Zhang, Yongsheng Chen, and Jian Guo Tian. Ultrafast carrier dynamics and saturable absorption of solution-processable few-layered graphene oxide. *Applied Physics Letters*, 98(12), mar 2011.

[6] E. K. Ng, K. Y. Lau, H. K. Lee, M. H. Abu Bakar, Y. Mustapha Kamil, M. F. Omar, and M. A. Mahdi. Saturable absorber incorporating graphene oxide polymer composite through dip coating for mode-locked fiber laser. *Optical Materials*, 100, 2020.

[7] Jia Xu, Jiang Liu, Sida Wu, Quan-Hong Yang, and Pu Wang. Graphene oxide mode-locked femtosecond erbium-doped fiber lasers. *Optics Express*, 20(14):15474, 2012.

[8] Byungjoo Kim, Seongjin Hong, Jaedeok Park, Yongsoo Lee, Dong-il Yeom, and Kyunghwan Oh. Laser-driven self-exfoliation of graphene oxide layers on a fiber facet for Q switching of an Er-doped fiber laser at the longest wavelength. *Photonics Research*, 8(8):1324, 2020.

[9] Y. K. Yap, N. M. Huang, S. W. Harun, and H. Ahmad. Graphene oxide-based Q-switched erbium-doped fiber laser. *Chinese Physics Letters*, 30(2), feb 2013.

[10] J. Liu, A. G. Rinzler, H. Dai, J. H. Hafner, R. K. Bradley, P. J. Boul, A. Lu, T. Iverson, K. Shelimov, and C. B. Huffman. Fullerene Pipes Jie. *Science*, 280(5367):1253–1256, 1998.

[11] Ray H. Baughman, Changxing Cui, Anvar A Zakhidov, Zafar Iqbal, Joseph N Barisci, Geoff M. Spinks, Gordon G. Wallace, Alberto Mazzoldi, Danilo De Rossi, Andrew G. Rinzler, Oliver Jaschinski, Siegmar Roth, and Miklos Kertesz. Carbon nanotube actuators. *Science*, 284(5418):1340–1344, 1999.

[12] Frank Hennrich, Sergei Lebedkin, Sharali Malik, Joseph Tracy, Matthias Barczewski, Harald Rösner, and Manfred Kappes. Preparation, characterization and applications of free-standing single walled carbon nanotube thin films. In *Physical Chemistry Chemical Physics*, volume 4, pages 2273–2277, 2002.

[13] Jonathan N Coleman, Werner J Blau, Alan B Dalton, Edgar Muñoz, Steve Collins, Bog G Kim, Joselito Razal, Miles Selvidge, Guillermo Vieiro, and Ray H Baughman. Improving the mechanical properties of single-walled carbon nanotube sheets by intercalation of polymeric adhesives. *Applied Physics Letters*, 82(11):1682–1684, mar 2003.

[14] L Berhan, Y B Yi, A M Sastry, E Munoz, M Selvidge, and R Baughman. Mechanical properties of nanotube sheets: Alterations in joint morphology and achievable moduli in manufacturable materials. *Journal of Applied Physics*, 95(8):4335–4345, apr 2004.

[15] Dmitriy A Dikin, Sasha Stankovich, Eric J Zimney, Richard D Piner, Geoffrey H.B. Dommett, Guennadi Evmenenko, Sonbinh T Nguyen, and Rodney S Ruoff. Preparation and characterization of graphene oxide paper. *Nature*, 448(7152):457–460, 2007.

[16] Junqing Zhao, Yonggang Wang, Peiguang Yan, Shuangchen Ruan, Yuen Tsang, Gelin Zhang, and Hui-

quan Li. An Ytterbium-doped fiber laser with dark and Q-switched pulse generation using graphene-oxide as saturable absorber. *Optics Communications*, 312:227–232, 2014.

[17] Ji Min Yang, Qi Yang, Jie Liu, Yong Gang Wang, and Yuen H. Tsang. Reflective graphene oxide absorber for passively mode-locked laser operating at nearly 1 μm. *Chinese Physics B*, 22(9), 2013.

[18] J I Paredes, S Villar-Rodil, A Martínez-Alonso, and J. M.D. Tascón. Graphene oxide dispersions in organic solvents. *Langmuir*, 24(19):10560–10564, oct 2008.

[19] A. Ferrari and J. Robertson. Interpretation of Raman spectra of disordered and amorphous carbon. *Physical Review B - Condensed Matter and Materials Physics*, 61(20):14095–14107, 2000.

[20] M. A. Pimenta, G. Dresselhaus, M. S. Dresselhaus, L. G. Cançado, A. Jorio, and R. Saito. Studying disorder in graphite-based systems by Raman spectroscopy, 2007.

[21] I. Calizo, A. A. Balandin, W. Bao, F. Miao, and C. N. Lau. Temperature dependence of the raman spectra of graphene and graphene multilayers. *Nano Letters*, 7(9):2645–2649, sep 2007.

[22] Keun Soo Kim, Yue Zhao, Houk Jang, Sang Yoon Lee, Jong Min Kim, Kwang S. Kim, Jong Hyun Ahn, Philip Kim, Jae Young Choi, and Byung Hee Hong. Large-scale pattern growth of graphene films for stretchable transparent electrodes. *Nature*, 457(7230):706–710, 2009.

[23] O Akhavan and E. Ghaderi. Escherichia coli bacteria reduce graphene oxide to bactericidal graphene in a self-limiting manner. *Carbon*, 50(5):1853–1860, 2012.

[24] Abhijit Ganguly, Surbhi Sharma, Pagona Papakonstantinou, and Jeremy Hamilton. Probing the thermal deoxygenation of graphene oxide using high-resolution in situ X-ray-based spectroscopies. *Journal of Physical Chemistry C*, 115(34):17009–17019, sep 2011.

[25] A Lerf, A Buchsteiner, J Pieper, S. Schöttl, I. Dekany, T. Szabo, and H. P. Boehm. Hydration behavior and dynamics of water molecules in graphite oxide. *Journal of Physics and Chemistry of Solids*, 67(5-6):1106–1110, 2006.

[26] Alexandra Buchsteiner, Anton Lerf, and Jörg Pieper. Water dynamics in graphite oxide investigated with neutron scattering. *Journal of Physical Chemistry B*, 110(45):22328–22338, nov 2006.

[27] Chen Y. Zhao C. J. Wang, Z.T. and H. Zhang. Switchable dual-wavelength synchronously Q-switched erbium-doped fiber laser based on graphene saturable absorber. *IEEE Photonics Journal*, 4(3):869–876, 2012.

[28] Orazio Svelto and Orazio Svelto. Properties of Laser. In *Principles of Lasers*, pages 475–504. Springer US, 2010.

[29] W. Y. Chong, Y. K. Yap, S Behameen, and H. Ahmad. Study of a high output coupling ratio Q-switched erbium-doped fibre laser using MoS2 saturable absorber. *Laser Physics*, 27(2), 2017.

[30] Laura J. Cote, Rodolfo Cruz-Silva, and Jiaxing Huang. Flash reduction and patterning of graphite oxide and its polymer composite. *Journal of the American Chemical Society*, 131(31):11027–11032, aug 2009.

[31] Maher F. El-Kady, Veronica Strong, Sergey Dubin, and Richard B. Kaner. Laser scribing of high-performance and flexible graphene-based electrochemical capacitors. *Science*, 335(6074):1326–1330, 2012.

[32] Victor Abdelsayed, Sherif Moussa, Hassan M Hassan, Hema S Aluri, Maryanne M Collinson, and M. Samy El-Shall. Photothermal deoxygenation of graphite oxide with laser excitation in solution and graphene-aided increase in water temperature. *Journal of Physical Chemistry Letters*, 1(19):2804–2809, oct 2010.

[33] Lei Huang, Yang Liu, Le Chun Ji, Yi Qun Xie, Tao Wang, and Wang Zhou Shi. Pulsed laser assisted reduction of graphene oxide. *Carbon*, 49(7):2431–2436, 2011.

[34] Honglei Guo, Mao Peng, Zhongming Zhu, and Lina Sun. Preparation of reduced graphene oxide by infrared irradiation induced photothermal reduction. *Nanoscale*, 5(19):9040–9048, 2013.

[35] H Ahmad, M. R. K. Soltanian, C. H. Pua, M. Alimadad, and S. W. Harun. Photonic crystal fiber based dual-wavelength Q-switched fiber laser using graphene oxide as a saturable absorber. *Applied Optics*, 53(16):3581, 2014.

[36] Sulaiman Wadi Harun, Muhamad Burhan Shah Sabran, Salam Mahdi Azooz, Ahmad Zarif Zulkifli, Mohd Afiq Ismail, and Harith Ahmad. Q-switching and mode-locking pulse generation with graphene oxide paper-based saturable absorber. *The Journal of Engineering*, 2015(6):208–214, jun 2015.

[37] Shinichi Watanabe. Basics of laser application to dermatology, 2008.

[38] M. M. Krasnov. Q-switched ("cool") lasers in ophthalmology. *International ophthalmology clinics*, 16(4):29–44, 1976.

[39] Vincent Delaye and Pierre Labeye. High-resolution eye-safe time-of-flight laser rangefinding. In *Laser Radar Technology and Applications V*, volume 4035, page 216, 2000.